

Strain Rate-dependent Model for Anisotropic Cohesive Soils

비등방성 점성토에 있어서 변형률속도 의존적 구성모델

Kim, Dae-Kyu*

김 대 규

요 지

지반의 실제 거동을 보다 정확하게 표현하기 위한, 응력의 비등방성 및 시간의존적(time-dependent) 거동의 적절한 묘사는 특히 점성토의 응력-변형률 관계를 나타내는 구성관계식에 있어서 중요한 관심사이다. 본 연구에서는 적은 모델정수로 응력의 비등방성을 묘사할 수 있는 소성 구성관계식과, 대표적 시간의존적 거동인 변형률속도 효과를 간편하게 표현할 수 있는 변형률속도 의존적 구성관계식을 일반 점성이론에 입각하여 조합하였다. 결론적으로 제안된 하나의 비등방성 변형률속도 의존적 구성관계식은 비교적 모델정수가 적고, 변형률속도가 바뀔 때마다 모델정수 값을 다시 결정할 필요가 없다는 장점이 있다. 제안된 구성모델은 인위적으로 제작된 균질한 시료를 이용한 실내시험을 통하여 검증되었으며, 상세 거동 및 문제점을 고찰하였다.

Abstract

The appropriate description of the stress-anisotropy and time-dependent behavior of cohesive soils is very important in representing the real soil behavior. In this study, two constitutive relations have been incorporated based on the generalized viscous theory: one is the plastic constitutive relation adopted to capture the stress-anisotropy with a few model parameters; the other is the rate-dependent constitutive relation adopted to describe the strain rate-dependent behavior, an important time-dependent behavior in cohesive soils. The incorporated and proposed constitutive model has relatively a few model parameters and their values need not to be re-evaluated at different strain rates. The proposed model has been verified and investigated with the anisotropic triaxial test results obtained by using the artificial homogeneous specimens.

Keywords : Constitutive relation, Strain rate-dependent, Stress-anisotropy, Time-dependent

1. Introduction

Modern constitutive relations try to precisely simulate, especially in cohesive soils, the stress anisotropy and time-dependent behavior. The stress anisotropy has been described in the form of the development of isotropic elastoplastic constitutive models. Constitutive model is evaluated in the consideration of certain theoretical background, the validity of mathematical formulation, the obvious identification and determination of the

model parameters, and the applicability(material and stress condition applied to). The determining procedure of the model parameters as well as their number and physical concepts might be most important in practical utilization of the model. The anisotropic elastoplastic models previously proposed have their own advantages and limitations in view of the above standard.

Such time-dependent behaviors of cohesive soils as creep, stress relaxation, and strain rate effect might be properly simulated with the viscous theory, not with the

* Member, Full-Time Instructor, Civil and Environ. Engrg., SangMyung Univ. (daekyu@smuc.ac.kr)

elastoplastic theory alone. Many constitutive models have been proposed based on the viscous theory. The viscous models also have advantages and limitations considering the evaluation criteria stated above. The general elasto-viscous theory proposed by Perzyna(1966) has been, in many cases, adopted for the time-dependent constitutive models since the theory has the merits of generality and practical usefulness. The models based on Perzyna's theory, however, mainly focus on the description of the creep and stress relaxation other than the strain rate effect.

In this study, two constitutive relations have been incorporated based on the Perzyna's generalized viscous theory. The model developed by Banerjee et al.(1986, 1988) was adopted as the plastic constitutive relation to capture the stress-anisotropy with few model parameters. The constitutive relation by Adachi et al.(1974, 1982) was used as the viscous relation. The model parameter values need not be re-evaluated under different strain rates. The combined and proposed constitutive model has the advantages of simulating the strain rate effect well with a few model parameters. The proposed model has been verified and investigated with the experimental results obtained by using the artificial homogeneous specimens. The concept of the theoretical background, mathematical formulation, and comparison with the experimental results are briefly presented in the following sections.

2. Development of the Constitutive Relation

The following eq. (1) was used for the development of the strain rate-dependent constitutive relation(Dafalias, 1982).

$$\dot{\epsilon}_{ij} = \dot{\epsilon}_{ij}^e + \dot{\epsilon}_{ij}^i = \dot{\epsilon}_{ij}^e + \dot{\epsilon}_{ij}^p + \dot{\epsilon}_{ij}^v \quad (1)$$

where the superscripts e, i, p, and v respectively represent elastic, inelastic, plastic, and viscous part, that is, total strain rate consists of elastic, plastic, and viscous strain rates.

2.1 Elastic, Plastic, Viscous Constitutive Relation

The elastic behavior is assumed to be strain rate-independent and to follow the generalized Hooke's law of eq. (2).

$$\dot{\epsilon}_{ij}^e = C_{ijkl} \dot{\sigma}_{kl} \quad (2)$$

The plastic behavior is represented by the associated flow rule of eq. (3)

$$\dot{\epsilon}_{ij}^p = \langle L \rangle \frac{\partial f}{\partial \sigma_{ij}} \quad (3)$$

The elastic, plastic, and viscous strain rates are independent and just superposed for total strain rate in the classical generalized elasto-visco-plasticity. In this study, the plastic behavior is assumed to be coupled with the viscous behavior for more precise simulation. The total strain rate, the elastic strain rate, and the plastic strain rate are respectively obtained by eq. (1), eq. (2), and eq. (3); however, the loading function L in eq. (3) is different from that in the classical plasticity. The loading function L in this study is obtained by the summation of the classical plastic loading function and the overstress function Φ . The viscous strain rate $\dot{\epsilon}_{ij}^v$ and the overstress function Φ are described in the viscous part.

The constitutive model proposed by Banerjee et al.(1986, 1988) is used to describe the plastic behavior in this study. In the model, the yield surface is assumed to be a distorted ellipsoid and the hardening rule adopted is a combination of isotropic and kinematic hardening rules(Fig. 1).

Due to the kinematic hardening, the material develops a new state of anisotropy at every stage of the loading process. The yield surface passes through the origin and intersects the failure surface as well as the hydrostatic stress axis. During a loading process, the yield surface rotates and the condition of $(\partial f / \partial \sigma_{ij})=0$ is automatically satisfied at the instant of failure. All formulations including the consistency condition and the obtaining procedure of the loading function L obey the classical plasticity.

Geotechnical processes and the stresses relevant to the

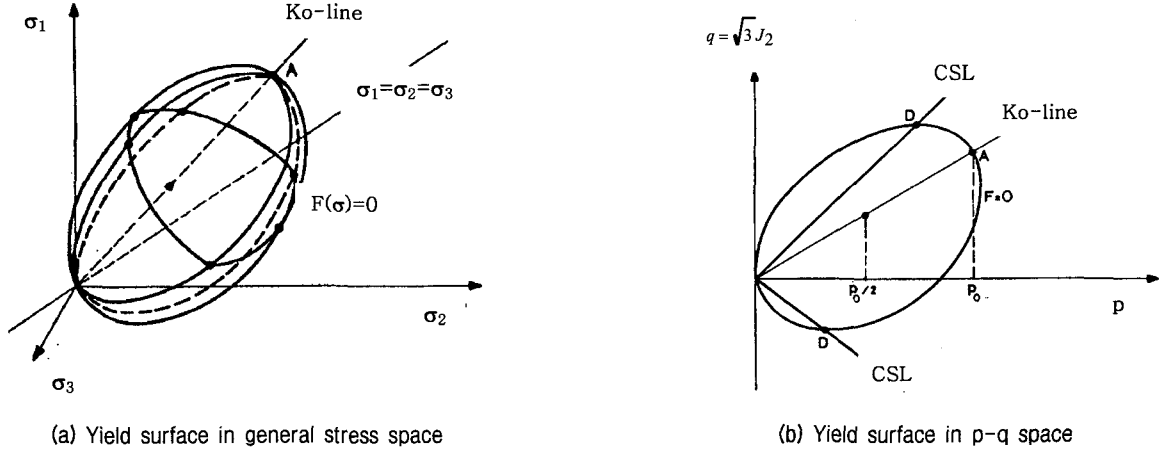


Fig. 1. Yield surface in general stress space and p-q space(Banerjee et al., 1986)

formation of naturally deposited soils are mainly responsible for the development of the inherent anisotropy. Subsequent application of a given stress history introduces further anisotropy, induced anisotropy, in the mechanical properties of real soils. The plastic model stated above has the advantage that it can account for both the inherent and induced anisotropy with relatively a few model parameters, which are the traditional λ (slope of virgin compression), κ (slope of unloading-reloading line), ν (poisson's ratio), ϕ (internal friction angle).

The viscous behavior is represented by eq. (4), based on the generalized viscous theory(Perzyna, 1966).

$$\dot{\epsilon}_{ij}^v = \langle \Phi \rangle \frac{\partial f}{\partial \sigma_{ij}} \quad (4)$$

where the overstress function Φ plays an important role in the plastic behavior through the coupling effect as well as the viscous behavior in the strain rate-dependent behavior of clays. Several forms of the overstress function have been proposed; however, eq. (5) by Katona (1984) has been widely and successfully used for geotechnical materials(Kaliakin, 1985; Kaliakin and Dafalias, 1990a, 1990b; Al-Shamrani and Sture, 1994).

$$\Phi = \frac{1}{V} \exp(J_2/N I_1) (\Delta \hat{\sigma})^n \quad (5)$$

$$\hat{V} = V \frac{1}{1 + \left\langle \left(\frac{2}{3} e_{ij}^i e_{ij}^i \right)^{0.5} - \epsilon_m \right\rangle} \quad (6)$$

where J_2 is the second invariant of the deviatoric stress

tensor, I_1 is the first invariant of the stress tensor, N is the slope of the critical state line in I_1 - J_2 space. $\Delta \hat{\sigma}$ is called normalized overstress and obtained through a closed form solution using the viscous nucleus parameter. s_v , e_{ij}^i is the inelastic deviatoric strain tensor and $\left\{ \left(\frac{2}{3} e_{ij}^i e_{ij}^i \right)^{0.5} \right\}$ is the accumulated inelastic deviatoric strain tensor. n , V , ϵ_m , and s_v are the model parameters related to the viscous behavior. To avoid the error appearing during the identification and value determination of the model parameters, constant values have been used for the \hat{V} in this study as in Kaliakin(1985).

Substituting eqs. (2) to (6) into eq. (1) produces a combined visco-elastoplastic constitutive relation. But in that case, a cumbersome work is needed to obtain the different values of the model parameters each time the strain rate changes. To make the problem more efficient, the overstress function proposed by Adachi et al.(1974, 1982) and Oka(1981, 1985) was used in this study.

2.2 Development of an Anisotropic Strain Rate-dependent Constitutive Relation

Adachi et al.(1974, 1982) and Oka(1981, 1985) proposed eqs. (7) to (9) based on the critical state energy theory(Roscoe and Burland, 1968).

$$\Phi = c_0 \exp[m' \ln((\sigma_{my}^{(d)} / \sigma_{my}^{(s)})] \quad (7)$$

static yield function :

$$\ln \sigma_{my}^{(s)} = f_s = \sqrt{2J_2^{(s)}} / N \sigma_m^{(s)} + \ln \sigma_m^{(s)} \quad (8)$$

dynamic yield function :

$$\ln \sigma_m^{(d)} = f_d = \sqrt{2J_2}/N\sigma_m + \ln \sigma_m \quad (9)$$

The static yield function means the initial yield function playing the role of the elastic nucleus in the classical plasticity. No viscous behavior occurred inside the static yield function. The dynamic yield function indicates the current yield function changing according to the hardening rules. In other words, the viscous behavior is described in the same way that the plasticity is described in the yield function and hardening rule. c_0 is the model parameter controlling the total magnitude of the overstress function but does not appear in the final form of the mathematical formulation as explained in eq. (18). m' is the model parameter determining the slope of the line connecting the maximum deviatoric stresses to the corresponding strain rates. σ_m is the mean principal stress. Eq. (7) can be expressed as eq. (10) using eqs. (8) and (9).

$$\Phi = c_0 \exp \left\{ m' \left[\frac{\sqrt{2J_2}}{N\sigma_m} + \ln \sigma_m - \frac{\sqrt{2J_2^{(s)}}}{N\sigma_m^{(s)}} - \ln \sigma_m^{(s)} \right] \right\} \quad (10)$$

The overstress function is rearranged, under triaxial condition, to eq. (11) using the principal stress difference $q = (\sigma_1 - \sigma_3)$ and the slope of the critical state line M in the mean principal stress- q space ($M = \sqrt{3/2}N$).

$$\Phi = c_0 \exp \left\{ m' \left[\frac{q}{M\sigma_m} + \ln \sigma_m - \frac{q^{(s)}}{M\sigma_m^{(s)}} - \ln \sigma_m^{(s)} \right] \right\} \quad (11)$$

Adachi and Oka(1982) proved that eq. (11) is valid under the undrained triaxial condition, based on the experimental results(Perzyna, 1966).

$$\dot{\epsilon}_{11} = \frac{\sqrt{2/3}}{N\sigma_m} \Phi \quad (12)$$

A relation between two different strain rates(strain rate (1) case, strain rate (2) case), under triaxial condition, can be expressed as eq. (13) from eqs. (11) and (12).

$$\ln \dot{\epsilon}_{11}^{(1)} = \ln \frac{\sqrt{2/3}}{N\sigma_m} + \ln c_0 + \left\{ m' \left[\frac{q^{(1)}}{M\sigma_m} + \ln \sigma_m - \frac{q^{(s)}}{M\sigma_m^{(s)}} - \ln \sigma_m^{(s)} \right] \right\} \quad (13)$$

$$\ln \dot{\epsilon}_{11}^{(2)} = \ln \frac{\sqrt{2/3}}{N\sigma_m} + \ln c_0 + \left\{ m' \left[\frac{q^{(2)}}{M\sigma_m} + \ln \sigma_m - \frac{q^{(s)}}{M\sigma_m^{(s)}} - \ln \sigma_m^{(s)} \right] \right\} \quad (14)$$

The relationship between two different strain rates is, using eqs. (13) and (14), as eq. (15) for the triaxial condition and as eq. (16) for the general stress condition.

$$\ln (\dot{\epsilon}_{11}^{(1)} / \dot{\epsilon}_{11}^{(2)}) = \frac{m'}{M} \times (q^{(1)} / \sigma_m - q^{(2)} / \sigma_m) \quad (15)$$

$$\ln (\dot{\epsilon}_{11}^{(1)} / \dot{\epsilon}_{11}^{(2)}) = \frac{m'}{N} \times (\sqrt{2J_2^{(1)}} / \sigma_m - \sqrt{2J_2^{(2)}} / \sigma_m) \quad (16)$$

where the superscripts (1) and (2) indicate strain rates (1) and (2), respectively. Eqs. (15) and (16) can be rearranged as eq. (17) on the basis of the second invariant of deviatoric stress tensor and using that the mean principal stress is one third of the first stress invariant.

$$J_2^{(2)} = \frac{1}{2} \left[\frac{N \times \sigma_m}{m'} \ln (\dot{\epsilon}_{11}^{(1)} / \dot{\epsilon}_{11}^{(2)}) - \sqrt{2J_2^{(1)}} \right]^2 = \frac{1}{2} \left[\frac{N \times \frac{1}{3} I_1}{m'} \ln (\dot{\epsilon}_{11}^{(1)} / \dot{\epsilon}_{11}^{(2)}) - \sqrt{2J_2^{(1)}} \right]^2 \quad (17)$$

The second invariant of deviatoric stress tensor at strain rate (2) can be, as shown in eq. (17), determined from the second invariant of deviatoric stress tensor at strain rate (1). Substituting eq. (17) into eq. (5), the overstress function is expressed as eq. (18).

$$\Phi = \frac{1}{\sqrt{V}} \exp \left(\frac{1}{2} \left[\frac{N \times \frac{1}{3} I_1}{m'} \ln (\dot{\epsilon}_{11}^{(1)} / \dot{\epsilon}_{11}^{(2)}) - \sqrt{2J_2^{(1)}} \right]^2 / NI_1 \right) (\Delta \hat{\sigma})^n \quad (18)$$

Substituting eq. (1) for eqs. (2), (3), (4), and (18), a strain rate-dependent constitutive relation is obtained. The overstress function, as stated above, effects the plastic behavior through the coupling as well as the viscous behavior. The model parameter values required and the verification of the proposed model are described in the following sections.

3. Laboratory Test

The anisotropic triaxial compression tests have been conducted to determine the values of the model parameters

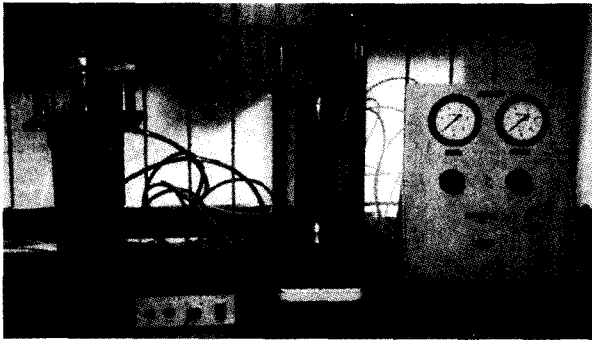


Fig. 2. Slurry consolidometer

and to compare the model predictions with the experimental results. A number of specimens with identical quality have been prepared, using the slurry consolidometer technique. They are very homogeneous with known stress history. To get the experimental results only by the strain rate difference, very homogeneous and reproducible specimen is essential, and the slurry consolidometer technique was very useful for the purpose as in the previous studies(Kurup et. al., 1994). Dry soils were, first, mixed with the deaired water, to be slurry, at twice the liquid limit. Then, the slurry was carefully placed into the consolidometer chamber(Fig. 2). The slurry was consolidated under K_0 condition and four steps of dead loadings. Fig. 3 represents the consolidation data of each loading step in the slurry consolidometer. After the slurry consolidation finished, the specimen was extracted and trimmed for the triaxial test. The slurry consolidometer was made of stainless steel and twice the triaxial specimen in diameter and height. The physical properties of the specimen is as in Table 1.

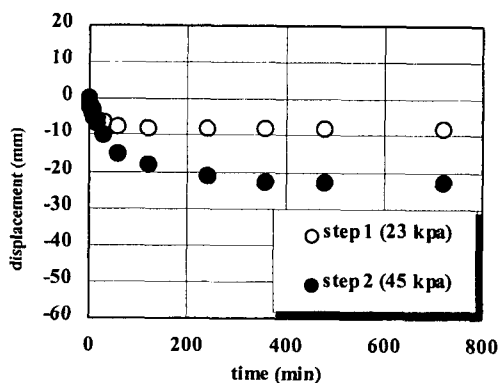


Table 1. Physical properties of specimen

ω_L (%)	45.0
ω_p (%)	25.0
PI	20
Gs	2.70
USCS	CL

Table 2. Triaxial test program

test	slurry consolidation σ'_v (kPa)	Ko consolidation in triaxial apparatus			strain controlled undrained shearing (%/min)
		σ'_v (kPa)	σ'_h (kPa)	σ'_h / σ'_v (kPa)	
1	176	200	98	0.49	0.1
2	176	200	98	0.49	0.01
3	176	200	98	0.49	0.001

Table 2 shows the triaxial test program conducted for determining the model parameter values and verifying the model. The only difference of the tests is the strain rate applied. Larger effective vertical stress than that in the slurry consolidometer was applied in the triaxial apparatus to remove the rigid boundary effect of the slurry consolidometer on the specimen.

4. Verification of the Developed Constitutive Model

Table 3 shows the values and determining method of the model parameters for the developed constitutive model.

The traditional critical state parameters λ , κ , ν , and

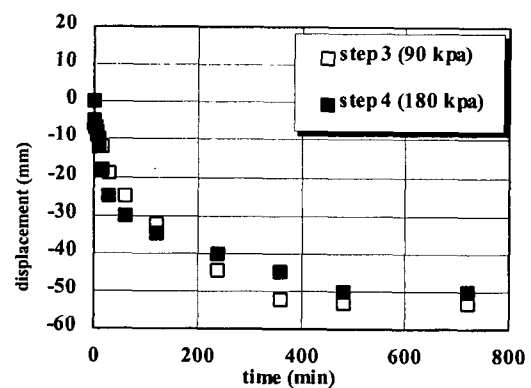


Fig. 3. Slurry consolidation of each loading step

Table 3. Model parameter values and determination

parameters		value	determination
slope of virgin compression	λ	0.34	triaxial test
slope of unloading-reloading	κ	0.067	triaxial test
internal friction angle	ϕ	24°	triaxial test
poisson's ratio	ν	0.3	assumed
viscous parameters	sv	2.0	fitting curves from triaxial test
	$\hat{\nu}$	40000	
	n	1.5	
rate-dependent parameter	m'	61	fitting curves from triaxial test
rate-dependent input	r	0.01	0.1%/min
	r	1	0.01%/min
	r	10	0.001%/min

ϕ are the elastoplastic model parameters related to Banerjee et al. (1986, 1988). The value of ν was assumed to be 0.3 and verified from the shear modulus G and Young's modulus E values obtained in triaxial tests. The viscous and rate-dependent parameters are involved in the overstress functions in eq. (18). s_v is the elastic nucleus parameter included in the image stress $\mathcal{A}\hat{\sigma}$ in eq. (18). m' is the slope of the line connecting the maximum deviatoric stress to the corresponding strain rate in deviatoric stress-strain rate space. The rate-dependent input r , not parameter but input, indicates $\dot{\varepsilon}_{11}^{(1)} / \dot{\varepsilon}_{11}^{(2)}$

in eq. (18). The values of all parameters were determined by fitting curves or directly from the triaxial test results performed at the standard strain rate 0.01%/min. Once the parameter values were determined, the values were used for the prediction at different strain rates, and only the input r changed as in Table 3.

Figs. 4 to 6 show the experimental results of the triaxial tests and the predictions using the developed constitutive model. The principal stress difference, the mean principal stress, and the undrained shear strength were normalized by the vertical consolidation stress, and respectively denoted by normalized q , normalized p' , and normalized s_u .

In Fig. 4, the maximum principal stress difference, as expected, increases with the increase of the strain rate. The model predictions show good agreement with the experimental results in all the three strain rates. The axial strain corresponding to the maximum principal stress difference is a little bit different from that of the model predictions. Best agreement appears at the strain rate of 0.01 %/min. since the model parameter values were determined from the experimental data at the strain rate. At the strain rate of 0.1%/min., the model prediction is higher than the experimental result, which might be due to the fact that the overstress function is overestimated at the higher strain rate. A model parameter, which can control the excessive overstress function, needs further research. At the strain rate of 0.001%/min., the model prediction matches well the experimental results in both

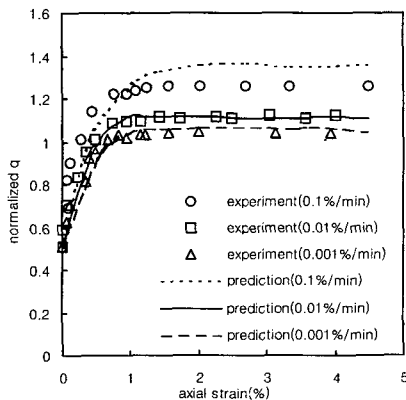


Fig. 4. Principal stress difference-axial strain with various strain rates

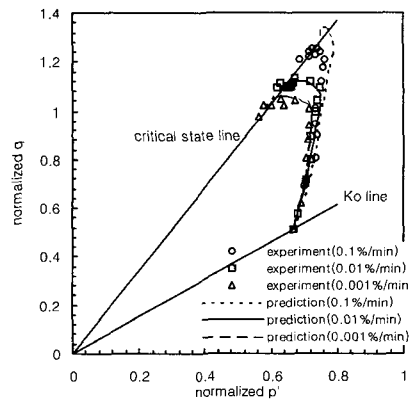


Fig. 5. Stress paths with various strain rates

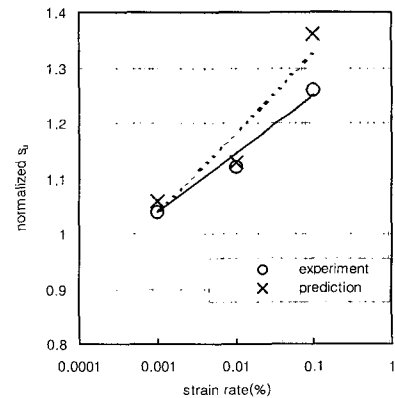


Fig. 6. Undrained shear strengths with various strain rates

the magnitude of the principal stress difference and the corresponding axial strain, in other words, the developed model gives better results at a lower strain rate than the standard strain rate. It may produce a future study in which the model parameter values are determined from the experimental data at a higher strain rate. Using more appropriate elastic model other than the generalized Hooke's law, would be anticipated to give better results in the initial part of the prediction.

Fig. 5 shows the stress paths. The model predictions represent very good agreement at strain rates of 0.01 and 0.001 %/min. like in the relationship between the normalized principal stress difference and the axial strain(Fig. 4). The predicted stress path at strain rate of 0.1 %/min. is also in the reasonable range compared with the experimental result. Fig. 6 indicates that undrained shear strength has a linear relationship to logarithmic strain rate, which confirms the viscous theory by Adachi et al.(1974, 1982) and Oka(1981, 1985) adopted in this study. It is unnecessary to re-evaluate the model parameter values at different strain rates in the developed model. Once the parameter values are determined at a strain rate, the values can be used at different strain rates. It is only the rate-dependent input r of the values in Table 3 which should be changed. The r is included in the overstress function. The overstress function seems to influence only the viscous strain rate, but it affects the plastic strain rate through the coupling(eq. 1).

5. Conclusions

In this study, the generalized Hooke's law, the plastic model proposed by Banerjee et al.(1986, 1988), and the viscous theory by Adachi et al.(1974, 1982) and Oka(1981, 1985) have been combined based on the generalized viscous theory by Perzyna(1966), to develop a strain rate-dependent constitutive model for anisotropic cohesive soils. The anisotropic triaxial compression tests have been conducted at the strain rates of 0.1, 0.01, 0.001 %/min. The homogeneous specimen was prepared using the slurry consolidometer technique. The model

prediction were compared with the triaxial experimental results, and showed good agreement specially at the strain rates of 0.01 and 0.001 %/min. A little larger prediction than the experimental results at the strain rate of 0.1 %/min is due to the overestimation of the overstress function. A parameter preventing from the excessive overstress function at higher strain rates needs further research. The developed constitutive model has a definite advantage that it is not necessary to re-evaluate the model parameter values each time the strain rate changes.

Acknowledgments

The writer acknowledge Kisun Lee for the help in the experiments.

References

1. Adachi, T., and Oka, F. (1982), "Constitutive Equations for Normally Consolidated Clay Based on Elasto-Viscoplasticity", *Soils and Foundations*, Japanese Geotechnical Society, Vol.22, No.4, pp.57-70.
2. Adachi, T. and Okano, F. (1974), "A Constitutive Equations for Normally Consolidated Clay", *Soils and Foundations*, Japanese Geotechnical Society, Vol.14, No.4, pp.55-73.
3. Al-Shamrani, M. A. and Sture, S. (1994), "Characterization of Time-dependent Behavior of Anisotropic Cohesive Soils", *Computer Methods and Advances in Geomechanics*, Siriwardane & Zaman (eds), pp.505-511.
4. Banerjee, P. K., Kumbhojkar, A. S. and Yousif, N. B. (1988), "Finite Element Analysis of the Stability of a Vertical Cut using an Anisotropic Soil Model", *Canadian Geotechnical Journal*, Vol.25, pp.119-127.
5. Banerjee, P. K. and Yousif, N. B. (1986), "A Plasticity Model for the Mechanical Behavior of Anisotropically Consolidated Clay", *Int. J. for Numerical and Analytical Methods in Geomechanics*, Vol.10, pp.521-541.
6. Dafalias, Y. F. (1982), "The Concept and Application of the Bounding Surface in Plasticity Theory, Physical non-linearities in Structural Analysis", *IUTAM Symposium*, Senlis, Francem J. Hult and J. Lemaitre, Eds., Springer Verlag, Berlin, pp.56-63.
7. Kaliakin, V.N. (1985), "*Bounding Surface Elastoplastic-Viscoplastic for clays*", Ph.D. Thesis, University of California at Davis, CA.
8. Kaliakin, V.N. and Dafalias, Y.F.(1990a), "Theoretical Aspect of the Elastoplastic-Viscoplastic Bounding Surface Model for Cohesive Soils", *Soils and Foundations*, Japanese Geotechnical Society, Vol.30, No.3, pp.11-24.
9. Kaliakin, V.N. and Dafalias, Y.F.(1990b), "Verification fo the Elastoplastic-Viscoplastic Bounding Surface Model for Cohesive

- Soils", *Soils and Foundations*, Japanese Geotechnical Society, Vol.30, No.3, pp.25-36.
10. Katona, M. G. (1984), "Evaluation of Viscoplastic Cap Model", *Journal of the Geotechnical Engineering*, ASCE., Vol.110, No.8, pp.1106-1125.
 11. Kurup, P. U., Voyiadjis, G. Z., and Tumay, M. T., (1994), "Calibration Chamber Studies of Piezocone Test in Cohesive Soils", ASCE, *J. of Geotechnical Engineering*, Vol.120, No.1, pp.81-107.
 12. Oka, F. (1981), "Prediction of Time Dependent Behavior of Clay", *Proceedings of the tenth International Conference on Soil Mechanics and Foundation Engineering*, Stockholm, Vol.1, pp.215-218.
 13. Oka, F. (1985), "Elasto/viscoplastic Constitutive Equations with Memory and Internal Variables", *Computers and Geotechnics*, Vol.1, pp.59-69.
 14. Perzyna, P. (1966), "The Constitutive Equations for Work Hardening and Rate Sensitive Plastic Materials", *Proc. Vibrational Problems*, Warsaw, Vol.4, No.3, pp.281-290.
 15. Roscoe, K. H. and Burland, J. B. (1968), "On the Generalized Stress-strain Behavior of Wet Clay", *Engineering Plasticity*, Cambridge University Press, pp.535-609.

(received on Oct. 29, 2002, accepted on Jun. 8, 2003)